



ELSEVIER

Biochimica et Biophysica Acta 1365 (1998) 363–372

BIOCHIMICA ET BIOPHYSICA ACTA

BBA

Detection of threonine structural changes upon formation of the M-intermediate of bacteriorhodopsin: evidence for assignment to Thr-89

Xiaomei Liu ^a, Min Joo Lee ^{1,a}, Matthew Coleman ^{2,a}, Parshuram Rath ^{3,a}, Anders Nilsson ^{4,a}, Wolfgang B. Fischer ^{5,a}, Marina Bizounok ^b, Judith Herzfeld ^b, Willem F. Jan Karstens ^c, Jan Raap ^c, Johan Lugtenburg ^c, Kenneth J. Rothschild ^{a,*}

^a *Physics Department and Molecular Biophysics Laboratory, Boston University, 590 Commonwealth Avenue, Boston, MA 02215, USA*

^b *Department of Chemistry and Keck Institute for Cellular Visualization, Brandeis University, Waltham, MA 02254, USA*

^c *Leiden Institute of Chemistry, University of Leiden, P.O. Box 9502, 2300 RA Leiden, Netherlands*

Received 10 March 1998; accepted 17 March 1998

Abstract

The behavior of threonine residues in the bacteriorhodopsin (bR) photocycle has been investigated by Fourier transform infrared difference spectroscopy. L-Threonine labeled at the hydroxyl group with ¹⁸O (L-[3-¹⁸O]threonine) was incorporated into bR and the bR → M FTIR difference spectra measured. Bands are assigned to threonine vibrational modes on the basis of ¹⁸O induced isotope frequency shifts and normal mode calculations. In the 3500 cm⁻¹ region, a negative band is assigned to the OH stretch of threonine. In the 1125 cm⁻¹ region, a negative band is assigned to a mixed CH₃ rock/CO stretch mode. The frequency of both these bands indicates the presence of at least one hydrogen bonded threonine hydroxyl group in light adapted bR which undergoes a change in structure by formation of the M intermediate. Spectral changes induced by the substitution Thr-89 → Asn but not Thr-46 → Asn or Asp-96 → Asn are consistent with the assignment of these bands to Thr-89. These results along with another related study on the mutant Thr-89 → Asn indicate that the active site of bR includes Thr-89 and that its interaction with the retinylidene Schiff base and Asp-85 may play an important role in regulating the color of bacteriorhodopsin and the transfer of a proton to the Schiff base. © 1998 Elsevier Science B.V. All rights reserved.

Keywords: Bacteriorhodopsin; Fourier transform infrared; Threonine; Proton transport; Site directed mutagenesis; Isotope labeling

Abbreviations: PM, purple membrane; bR, bacteriorhodopsin; IR, infrared; FTIR, Fourier transform infrared; a.u., absorbance units; L-[3-¹⁸O]threonine, L-threonine labeled at the hydroxyl group with ¹⁸O; [3-¹⁸O]Thr bR, bacteriorhodopsin containing L-[3-¹⁸O]threonine

* Corresponding author. Fax: +1 (617) 353-5167.

¹ Present address: Plant Cell Biology, Lund University, Box 7007, S-220 07 Lund, Sweden. Permanent address: Department of Chemistry, Changwon National University, Changwon, Kyungnam 641-773, South Korea.

² Present address: Lawrence Radiation Laboratories, 7000 East Ave., Livermore, CA 94551, USA.

³ Present address: Emisphere Technologies, Inc., 15 Skyline Dr., Hawthorne, NY 10532, USA.

⁴ Present address: Plant Cell Biology, Lund University, Box 7007, S-220 07 Lund, Sweden.

⁵ Present address: Institut für Analytische Chemie, Technische Universität, 01062 Dresden, Germany.

1. Introduction

Bacteriorhodopsin (bR) is the light-driven proton pump found in the purple membrane of *Halobacterium salinarium*. Like rhodopsin, the photoreceptor in vision, bR contains a retinylidene chromophore linked to a lysine residue (Lys-216) through a protonated Schiff base [1,2]. Because of bR's relatively low molecular weight (26 000 kDa), availability in large quantities, stability over a wide range of temperatures and crystallization into a 2-dimensional lattice, it has become an important model for studying proton transport and energy transduction in biomembranes [3–7]. In addition, the discovery of similar membrane proteins from *H. salinarium* which exhibit receptor function (sensory rhodopsins I and II) [8] and active chloride transport (halorhodopsin) [9,10] has broadened interest in this system beyond proton transport.

Upon absorption of light, bR undergoes a photocycle with intermediate states characterized by absorption λ_{\max} values as follows:



One approach to investigating this photocycle is the use of Fourier transform difference infrared spectroscopy [11–15]. Infrared spectra are recorded for specific states of the bR molecule (e.g. bR_{568} and M_{412}) by using either low temperature or time resolved methods, and the difference between the initial and light induced spectrum is computed. These difference spectra contain detailed information about conformational changes occurring in the protein and retinylidene chromophore during the photocycle. Furthermore, it is possible through a combination of isotope substitution and site-directed mutagenesis to assign specific bands in the FTIR difference spectrum to individual amino acid residues [12,16–18]. This information, along with results from other molecular level probes such as solid-state NMR [19] and resonance Raman spectroscopy [20,21] has provided a basis for constructing an increasingly detailed model of the bR proton pump mechanism.

Although bands from a number of residues, including Tyr, Asp and Trp, have been previously assigned in FTIR difference spectra of bR, thus far no vibrations due to threonine residues have been identified. More generally, no vibrations due to threonine

changes have yet been identified in any protein by FTIR difference spectroscopy. In bR, at least two threonine residues, Thr-46 and Thr-89, might be expected to undergo changes during the bR photocycle on the basis of several recent structure–function studies. For example, it was concluded that Thr-46 interacts with Asp-96, the Schiff base proton donor due to changes detected in the environment of Asp-96 in the mutant T46V [22]. It was also found that Asp-46 can substitute for Asp-96 as the Schiff base proton donor [22]. Changes in water molecules located in the Asp-96/Thr-46 domain during formation of the L intermediate have also been detected [23,24]. In the case of Thr-89, red-shifts in the λ_{\max} of the mutants T89D, T89A have been reported [22]. More recently, studies of the mutant T89N, which also exhibits a red-shifted λ_{\max} , indicate that Thr-89 interacts with both the retinylidene Schiff base and Asp-85, the Schiff base proton acceptor during the bR photocycle [25]. Previously, it has been suggested that Thr-89 participates in proton transfer from Asp-96 to the Schiff base during the M \rightarrow N transition, either by directly transferring a proton to the Schiff base [26], or through other intermediate residues which are part of a hydrogen bonded network such as Tyr-185 and Asp-212 [27].

In this paper we have further examined the possibility that one or more threonines are active in bR photocycle by using isotope labeling and site-directed mutagenesis to identify changing threonine residues. We find two negative bands in the bR \rightarrow M difference spectrum of bR near 3500 and 1125 cm^{-1} which are sensitive to ^{18}O substitution of the hydroxyl group of threonine. Normal mode calculations on the model compound 2-propanol show that these bands correspond to the OH stretch and CO stretch/ CH_3 rock, respectively, of a threonine side-chain with hydrogen bonding at the hydroxyl group. A tentative assignment of these bands to Thr-89 is made on the basis of changes observed in these bands for the mutant T89N but not T46N.

2. Materials and methods

2.1. Expression of T89N, T46N, T46N/T89N

Mutants of bacteriorhodopsin were expressed in

H. salinarium. All methods and procedures were previously described [27,28]. Wild type (WT) and mutant strains were grown, and the purple membrane was isolated, using previously described procedures [29]. The desired mutations in the *bop* gene were verified by sequencing prior to and after expression.

2.2. Isotope labeling

L-[3-¹⁸O]Threonine was synthesized and incorporated in bacteriorhodopsin as described previously which resulted in approximately two-thirds of the threonine residues labeled, with no scrambling [23]. [Indole-¹⁵N]tryptophan-labeled bacteriorhodopsin was obtained by biosynthetic incorporation of ¹⁵N-anthranilic acid (ICON, Summit, NJ) as reported previously [30].

2.3. FTIR difference spectroscopy

bR → M FTIR difference spectra were recorded using previously reported methods [16,31]. Samples were prepared by air-drying approximately 100–200 μg/cm² of sample on a AgCl window and then rehydrating prior to insertion into a sealed transmittance cell which was mounted in a Helitran cryostat (Air Products, Allentown, PA). The water content of the sample was checked by monitoring the 3400 cm⁻¹ peak. All samples, except where noted, were light-adapted at room temperature prior to cooling by illuminating the sample for at least 15 min with a 150 W tungsten light source (Dolan-Jenner Industries, Lawrence, MA) equipped with a 505 nm long-pass filter. Spectra were recorded at 2 cm⁻¹ resolution and 250 K using a Nicolet Analytical Instruments 740 spectrometer (Madison, WI).

2.4. Normal mode analysis

In order to analyze the normal modes of threonine, calculations were performed with the Gaussian-94 program [32] using the BLYP/6-31G(d) basis set. This allowed for calculation of the force constants, infrared intensities, and vibrational frequencies for both the stable *gauche* (hydrogen atom of hydroxyl group *gauche* to the hydrogen atom of the 2-carbon) and *trans* (hydrogen atom of hydroxyl group *trans* to the hydrogen atom of 2-carbon) con-

figurations of 2-propanol and [3-¹⁸O]2-propanol. The Cartesian coordinates obtained for the optimized structures were input into the G-matrix program together with the internal coordinates. The B-matrix, which is the output of G-matrix program, was used to convert the calculated force constants in Cartesian coordinates to force fields in internal coordinates. All diagonal elements of the force field were obtained using scaling factors. This force field and symmetry coordinates, which are the same as with those used previously [33], were input into the F-matrix program. Initially, all scaling factors were kept fixed at 1.0 to produce the pure calculated vibrational frequencies and the potential energy distributions (PEDs). Subsequently, scaling factors were obtained by comparing the calculated and observed frequencies of the infrared spectra of the gaseous state of 2-propanol [33] and utilized to obtain the scaled force field and the resultant frequencies.

3. Results

3.1. Effects of L-[3-¹⁸O]threonine label

3.1.1. The 1800–1000 cm⁻¹ region

The bR → M FTIR difference spectra of WT and [3-¹⁸O]threonine-bR were recorded at 250 K using steady-state illumination (Fig. 1). Under these conditions, WT exhibits spectral differences which primarily reflect the depletion of light-adapted bR (bR₅₆₈) and formation of the M intermediate [31]. For example, negative bands assigned to the vibrational modes of the light-adapted bR chromophore appear at 1640 cm⁻¹ (C=N stretch of protonated Schiff base) and 1527 cm⁻¹ (ethylenic C=C stretch), whereas a positive band appears at 1762 cm⁻¹ assigned to the C=O stretch mode of Asp-85 [16]. We also note that bands characteristic of the bR → N transition such as at 1755 (+), 1670 (-) and 1186 (+) cm⁻¹ [34,35] are weak or not detectable.

As seen in Fig. 1, the difference spectrum of WT and [3-¹⁸O]Thr-bR are very similar with almost no noticeable changes at the scale of 10⁻³ a.u. However, at higher magnification (Fig. 2) the region from 1100 to 1150 cm⁻¹ shows reproducible differences for [3-¹⁸O]Thr-bR. Two independently recorded spectra

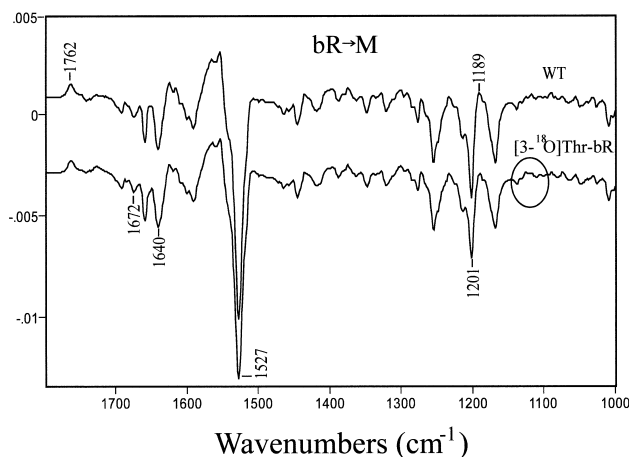


Fig. 1. bR \rightarrow M FTIR difference spectra of WT and $[3-^{18}\text{O}]\text{Thr-bR}$. Spectra were recorded at 250 K with 2 cm^{-1} resolution, using steady state illumination (see Section 2). The bR spectrum was subtracted from the M spectrum so that positive bands represent features of M not present in bR and negative bands represent features in bR not present in M. The y-scale markings, in a.u., are for the WT difference spectrum. The circled area indicates the region where $[3-^{18}\text{O}]\text{Thr}$ induced isotope shifts were observed.

are shown for the labeled bR to illustrate the reproducibility of the band changes, with the 1125 cm^{-1} band becoming more intense relative to the 1117 cm^{-1} band. In contrast, WT bR \rightarrow M difference spectra exhibit a more intense 1117 cm^{-1} band as shown in Fig. 2 and in other published spectra [31]. Furthermore, these changes cannot be attributed to alterations in the photostationary composition of the sample, since the two samples shows very similar spectra in other regions (Fig. 1). A similar change in intensity near 1125 cm^{-1} also occurs for WT hydrated in D_2O . One possibility consistent with this data is that a negative band in WT located near 1125 cm^{-1} undergoes an isotopic downshift in $[3-^{18}\text{O}]\text{Thr-bR}$, although the exact amount of the downshift is difficult to determine due to the baseline drift at lower frequency (see Fig. 2, top).

3.1.2. The $3300\text{--}3700\text{ cm}^{-1}$ region

In general, the region above 3200 cm^{-1} reflects OH and NH stretch vibrations, including modes from peptide groups (amide A, NH stretch), amino acid side chains with NH containing groups such as tryptophan (indole NH stretch), water (OH stretch) and other hydroxyl containing residues such as serine and threonine (OH stretch). As seen in Fig. 3, several

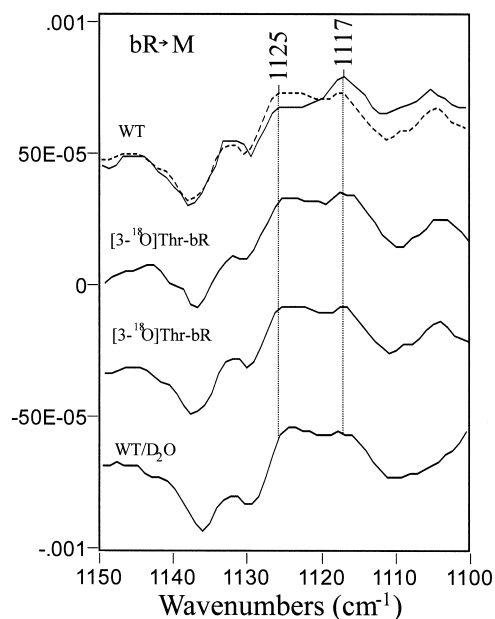


Fig. 2. bR \rightarrow M FTIR difference spectra of WT, $[3-^{18}\text{O}]\text{Thr-bR}$ and WT hydrated in D_2O . Difference spectra in the region from 1100 to 1150 cm^{-1} were recorded as described in Fig. 1. Spectra from two different samples of $[3-^{18}\text{O}]\text{Thr-bR}$ are shown. The y-scale markings, in a.u., are for the $[3-^{18}\text{O}]\text{Thr-bR}$ difference spectrum.

bands appear in this region for the bR \rightarrow M difference spectrum. The negative/positive bands at $3642/3665\text{ cm}^{-1}$ band have been previously assigned on

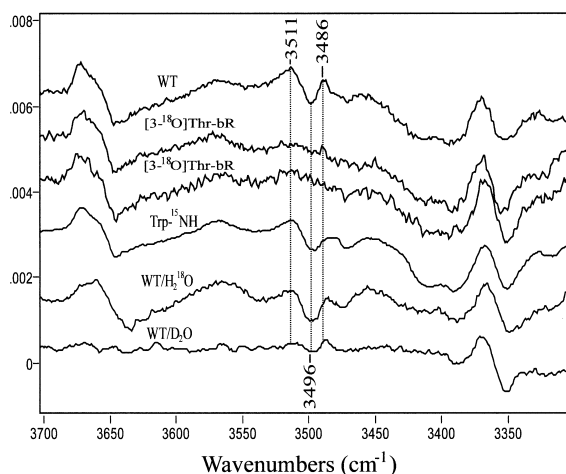


Fig. 3. bR \rightarrow M FTIR difference spectra of WT, $[3-^{18}\text{O}]\text{Thr-bR}$, $[\text{indole-}^{15}\text{N}]\text{tryptophan-labeled bacteriorhodopsin}$, WT hydrated in H_2^{18}O and WT hydrated in D_2O . Difference spectra were recorded as described in Fig. 1. The y-scale markings, in a.u., are for the WT difference spectrum.

the basis of an H_2^{18}O induced frequency shift of $\sim 12\text{ cm}^{-1}$ (Fig. 3) to a weakly hydrogen bonded water molecule which undergoes a further decrease in hydrogen bonding during M formation [36,37].

A comparison of the difference spectra from WT and $[3\text{-}^{18}\text{O}]\text{Thr-bR}$ (Fig. 3) shows that the OH stretch mode of the threonine hydroxyl group also contributes to this region. In particular, the bands in WT at 3511 (+), 3496 (–) and 3486 (+) cm^{-1} are largely absent in $[3\text{-}^{18}\text{O}]\text{Thr-bR}$, replaced by a less intense and broader band in this region, centered near 3510 cm^{-1} . Since an ^{18}O label is expected to cause a $\sim 10\text{--}12\text{ cm}^{-1}$ downshift in the frequency of the OH stretch mode (see below and Table 1), the bands in this region are not expected to completely disappear. An intense band at 3486 cm^{-1} was previously assigned in the $\text{bR} \rightarrow \text{L}$ difference spectrum to the N–H stretching vibration of the indole tryptophan on the basis of [indole- ^{15}N]tryptophan labeling [30]. As seen in Fig. 3, the much smaller band at 3486 cm^{-1} in the bRM difference spectrum must also be due to the N–H stretch of an indole tryptophan, since [indole- ^{15}N]tryptophan labeling causes a downshift to 3477 cm^{-1} . Thus, it is likely that the negative band

at 3496 cm^{-1} arises from the OH stretch mode of a threonine and downshifts upon $[3\text{-}^{18}\text{O}]\text{Thr}$ labeling, thereby canceling the band at 3486 cm^{-1} due to tryptophan.

Since the positive band at 3511 cm^{-1} is also reduced in intensity in $[3\text{-}^{18}\text{O}]\text{Thr-bR}$, it is likely to have some contributions from a threonine residue. Its presence along with the appearance of the negative band at 3496 cm^{-1} could indicate that the threonine hydroxyl group undergoes a decrease in hydrogen bond strength upon M formation. However, the presence of residual intensity in this region and absence of a clear downshift makes its assignment less certain. We also note that the bands at 3511 and 3496 cm^{-1} disappear for WT in D_2O as expected if the threonine hydroxyl group is accessible to water. In contrast, a small band is still discernible at 3486 cm^{-1} , in agreement with an earlier conclusion that the tryptophan NH group is inaccessible to water [30].

3.2. Effects of site-directed mutagenesis

Figs. 4 and 5 compare the $1100\text{--}1150$ and $3300\text{--}3700\text{ cm}^{-1}$ regions, respectively, for WT, $[3\text{-}^{18}\text{O}]\text{Thr-bR}$ and various mutations at Thr-89, Thr-46 and Asp-96. As seen in Fig. 4, the mutant T89N has similar spectral change as $[3\text{-}^{18}\text{O}]\text{Thr-bR}$, with an increase in the intensity of the 1125 cm^{-1} band rel-

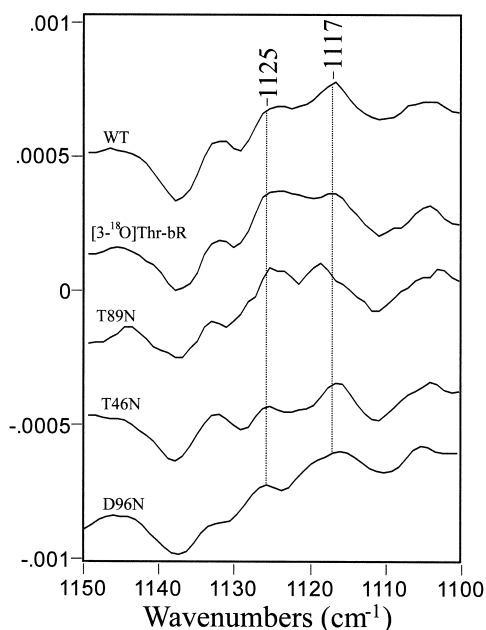


Fig. 4. $\text{bR} \rightarrow \text{M}$ FTIR difference spectra of WT, $[3\text{-}^{18}\text{O}]\text{Thr-bR}$ and the mutants T89N, T46N and D96N. Difference spectra were recorded as described in Fig. 1. The y-scale markings, in a.u., are for the $[3\text{-}^{18}\text{O}]\text{Thr-bR}$ difference spectrum.

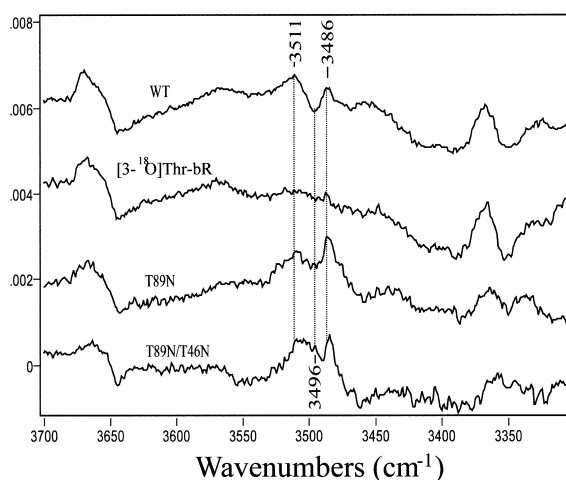


Fig. 5. $\text{bR} \rightarrow \text{M}$ FTIR difference spectra of WT, $[3\text{-}^{18}\text{O}]\text{Thr-bR}$ and the mutants T89N, T89N/T46N. Difference spectra were recorded as described in Fig. 1. The y-scale markings, in a.u., are for the WT difference spectrum.

Table 1

Observed and calculated frequencies (cm^{-1}), infrared intensities, and potential energy distribution (PED) for some bands of 2-propanol

Frequency								Description (PED)		
$^{16}\text{O-H}$ 2-propanol		$^{18}\text{O-H}$ 2-propanol		$^{16}\text{O-H}$ 2-propanol		$^{18}\text{O-H}$ 2-propanol		Observed ^c		
BLYP/ 6-31G(d) ^a	Fixed scaled ^b	BLYP/ 6-31G(d) ^a	Fixed scaled ^b	BLYP/ 6-31G(d) ^a	Fixed scaled ^b	BLYP/ 6-31G(d) ^a	Fixed scaled ^b	Gas	Liquid	
<i>Gauche</i>										
3573 (1.1)	3661	3562 (0.9)	3650	3459 (0.6)	3544	3447 (0.6)	3533	3665	3345	100% OH stretch
1130 (22.9)	1130	1126 (20.9)	1126	1130 (22.7)	1130	1126 (20.8)	1126	~ 1140	1130	45% CH ₃ rocks, 22% CO 10% 2-CH in-plane bend
<i>Trans</i>										
3553 (1.3)	3641	3542 (1.2)	3629	3439 (0.8)	3524	3428 (0.7)	3513			
1117 (17.4)	1117	1116 (17.1)	1116	1117 (17.5)	1117	1116 (17.1)	1116			100% OH stretch 46% CCC asym- metric stretch, 31% CH ₃ rocks, 12% skeletal bend III

^aNumbers in parentheses are calculated infrared intensities in km mol^{-1} .

^bCalculated using scaling factors of 1.050 for OH stretch and 1.0 for others.

^cValues from the infrared spectra of 2-propanol [33].

ative to the 1117 cm^{-1} band. This further indicates that a negative band is located at 1125 cm^{-1} which most likely arises from Thr-89. In contrast, the T46N and D96N mutants are more similar to the WT spectrum in this region making it unlikely that either of these residues is involved in the $[3-^{18}\text{O}]\text{Thr}$ associated spectral changes.

A similar conclusion can also be drawn from the spectral changes induced by mutations near 3500 cm^{-1} , as shown in Fig. 5. In the case of T89N, the negative band at 3496 cm^{-1} disappears, although not the 3511 cm^{-1} or the 3486 cm^{-1} bands, which increase in the intensity. This effect can be explained by the disappearance of the negative band at 3496 cm^{-1} , which in wild type partially cancels the positive band at 3486 cm^{-1} . Although the 3511 cm^{-1} band is not reduced in intensity, it still may have contribution from Thr-89, since the removal of the negative band at 3496 cm^{-1} would tend to increase its intensity, which is not observed. Although, insufficient signal/noise was obtained for T46N (data not shown), the double mutant T89N/T46N resembles

T89N indicating that Thr-46 does not contribute significantly to this region. We also note that the T89N mutation does not alter the bands at $3642/3665$ assigned to a water molecule, indicating that this water is not likely to interact with Thr-89.

3.3. Normal vibrational modes of threonine

In order to tentatively assign the bands near 3500 and 1125 cm^{-1} to specific threonine vibrations, the normal modes of the model compound 2-propanol and the isotope analog ($[3-^{18}\text{O}]\text{2-propanol}$) were calculated for both the *gauche* and *trans* configurations (see Section 2). The modes, first determined with the force constants obtained by density functional theory calculations using the BLYP/6-31G(d) basis level, were scaled to match the frequencies of the OH stretch (3665 cm^{-1}) of 2-propanol in the gas phase and then further adjusted to account for hydrogen bonding by lengthening the OH bond in order to fit the 3500 cm^{-1} band (increase of 0.009 \AA). Table 1 shows that the frequency of this mode for both the

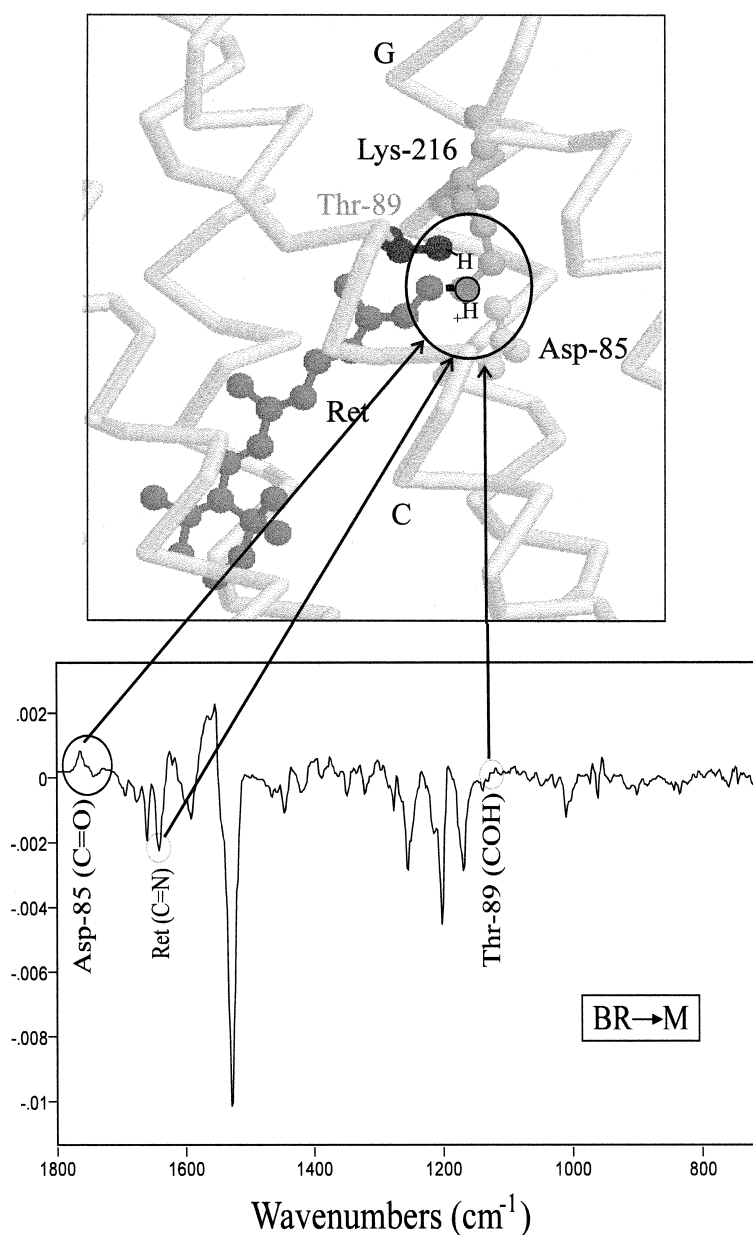


Fig. 6. Structural model of bR from electron diffraction derived coordinates and bR \rightarrow M FTIR difference spectrum of WT. Key residues in the retinal binding pocket are shown (Thr-89 and Asp-85 on the C helix and Lys-216 on the G helix) [3]. Ret denotes the all-*trans* retinylidene chromophore. The distance between the oxygen of the Thr-89 hydroxyl group and the nearest oxygen of the Asp-85 carboxylate group is 3.1 Å. Arrows connect to corresponding bands assigned in the bR \rightarrow M FTIR difference spectrum, including the tentative assignment to Thr-89. Note that the position of the hydrogen atoms 'H' shown are not specified in the electron diffraction structure and represent only the hypothesized positions in the model.

gauche and *trans* isomers downshifts by approximately 11 cm^{-1} upon ^{18}O labeling in agreement with our measurements. Table 1 also shows that the addition of hydrogen bonding through an increase in the OH bond distance shifted the OH stretch mode of both isomers into the 3500 cm^{-1}

region. Thus, we assign the isotope sensitive negative band near 3500 cm^{-1} to the OH stretch mode of a threonine residue which is hydrogen bonded.

A similar picture also arises from normal mode analysis of the band near 1125 cm^{-1} . In this case, the closest mode, which consisted of mixed motions

of several groups including the C–O (stretch), CH₃ (rock), and CH (in-plane band), was found at 1130 cm⁻¹ for the *gauche* configuration of 2-propanol (1). This mode shifted from 1130 to 1126 cm⁻¹ upon ¹⁸O labeling due to involvement of the C–O stretch. A 3 cm⁻¹ shift was also found due to substitution of the OH group with OD (data not shown). The frequency of no other mode calculated for 2-propanol showed as strong an ¹⁸O-isotope sensitivity in this region. In contrast to the *gauche* configuration of 2-propanol, the corresponding mode calculated for the *trans* isomer (1) had a frequency of 1117 cm⁻¹ and was less sensitive to ¹⁸O labeling (1 cm⁻¹ downshift). This decreased isotope effect arises due to the smaller involvement of the CO stretch motion in the *trans* configuration of threonine. It was also found that increased hydrogen bonding as modeled by changing the length of the OH bond (see above) did not significantly shift the frequency of these bands for both the *gauche* and *trans* configurations of 2-propanol. Thus, one possible explanation for our results is that the isotope sensitive negative band near 1125 cm⁻¹ arises from the CH₃ rock and CO stretch mixed mode of threonine in the *gauche* form. However, this explanation should be considered tentative until a more complete normal mode analysis can be performed on a larger molecule which better models all of the vibrational modes of threonine.

4. Discussion

Vibrational modes of a threonine residue involved in a conformational change of a protein have not been previously detected by FTIR difference spectroscopy. The current work establishes that at least one threonine residue in bacteriorhodopsin undergoes some type of structural/environmental change upon formation of the M intermediate. Although we cannot yet determine the exact nature of this change, normal mode analysis of the model compound 2-propanol indicates that the observed changes are likely to involve the COH group of threonine. In view of the identification of two negative bands, this may indicate either a partial deprotonation of one or more threonine COH groups or a change in hydrogen bonding (where the expected positive bands are masked).

Based on FTIR measurements of a limited set of bR mutants involving Thr-46 and Thr-89, the most likely candidate for the threonine which is altered during the bR → M transition is Thr-89. Since there are 18 threonines in bacteriorhodopsin, a definitive assignment would require examination of mutants for each of these threonines as performed previously for tyrosines [38] or alternatively site-directed isotope labeling as recently demonstrated for the case of tyrosine [39]. However, a previous study where all 15 threonines in the bilayer region of bR were changed to valine showed that only Thr-46, Thr-89, Thr-90 mutants had significantly perturbed phenotypes [40]. Of these three, Thr-89, exhibited the largest changes, with the λ_{\max} shifting from 560 to 414 nm when a valine was substituted, indicating a significant alteration in protein structure. We therefore consider Thr-89 the most likely assignment for the threonine bands identified in the bR → M difference spectrum by isotope labeling. Although not discussed here, threonine bands have also been identified in the b → RK and b → RL difference spectra (our unpublished data).

The detection of structural changes in Thr-89 during the bR photocycle is also consistent with information about its location in bR. As seen in the electron diffraction derived structural model of bR [3] (Fig. 6), the Thr-89 oxygen is only 3.8 Å from the Schiff base nitrogen and 3.1 Å from an oxygen on the Asp-85 carboxylic acid group. Thus, it is in a position to be influenced by, and participate in, changes in the bR active site which occur during the photocycle. For example, during the L → M step of the photocycle, a proton is transferred from the Schiff base to Asp-85 [16]. This may alter the charge balance in the active site and cause the release of a proton to the extracellular medium [16], possibly through the involvement of Arg-82 and Glu-204 [41–43]. Asp-85 also participates in the hydrogen-bonded complex that constitutes the Schiff base counterion, and influences the visible absorption of bacteriorhodopsin and its photointermediates.

In agreement with the possibility that Thr-89 participates in the active site, a recent study [25] reveals that the Thr-89 to Asn substitution (T89N) red-shifts the λ_{\max} to 582 nm and downshifts the C=N and C=C stretch of the chromophore. In addition, T89N as well as the double mutant T46N/T89N exhibit an

altered hydrogen bonding of the Asp-85 carboxylic acid group in the M intermediate as indicated by a 10 cm^{-1} downshift in frequency from 1762 cm^{-1} to 1752 cm^{-1} (see Fig. 5 of Ref. [25]). Finally, the T89N substitution interferes with transfer of a proton from the Schiff base during M formation, but does not appear to affect Schiff base reprotonation.

It is interesting to note that along with the newly identified threonine bands, the Asp-85 carboxyl group and the Schiff base vibrations also appear in FTIR difference spectrum (Fig. 6, lower panel), providing unique spectroscopic markers to monitor changes of three interacting groups (Thr-89, Asp-85 and the Schiff base) which may be located within a 4 \AA sphere. Polarized FTIR difference spectroscopy should provide additional information about the orientation of these groups at different steps in the photocycle while time-resolved FTIR difference spectroscopy should extend these measurements to shorter time ranges and samples at room temperature.

Acknowledgements

We wish to thank Drs. J. Olejnik, S. Williams and L. Smilowitz for helpful discussions. This work was supported by a grant from the NSF (MCB9419059) to K.J.R. and from the NIH (GM36810) to J.H. A.N. is supported by a postdoctoral fellowship from the Wenner-Gren Center Foundation (Sweden). M.C. is supported by an NIH Molecular Biophysics Training Grant (GM08291-06).

References

- [1] H. Bayley, R. Radhakrishnan, K.-S. Huang, H.G. Khorana, *J. Biol. Chem.* 256, (8) (1981) 3797–3801.
- [2] K.J. Rothschild, P.V. Argade, T.N. Earnest, K.S. Huang, E. London, M.J. Liao, H. Bayley, H.G. Khorana, J. Herzfeld, *J. Biol. Chem.* 257 (1982) 8592–8595.
- [3] N. Grigorieff, T.A. Ceska, K.H. Downing, J.M. Baldwin, R. Henderson, *J. Mol. Biol.* 259 (1996) 393–421.
- [4] M.P. Krebs, H.G. Khorana, *J. Bacteriol.* 175 (1993) 1555–1558.
- [5] J.K. Lanyi, *Biochim. Biophys. Acta* 1183 (1993) 241–261.
- [6] K.J. Rothschild, S. Sonar, in: W.M. Horspool, P.-S. Song (Eds.), *CRC Handbook of Organic Photochemistry and Photobiology*, CRC Press, London, 1995, pp. 1521–1544.
- [7] W. Stoeckenius, R.A. Bogomolni, *Annu. Rev. Biochem.* 51 (1982) 587–616.
- [8] J.L. Spudich, R.A. Bogomolni, *Annu. Rev. Biophys. Biophys. Chem.* 17 (1988) 193–215.
- [9] J. Lanyi, *Physiol. Rev.* 70 (1990) 319–329.
- [10] D. Oesterhelt, J. Tittor, E. Bamberg, *J. Bioenerg. Biomembr.* 24 (1992) 181–191.
- [11] K. Gerwert, B. Hess, *Mikrochim. Acta* (1988) (in press).
- [12] A. Maeda, *Israel J. Chem.* 35 (1995) 387–400.
- [13] K.J. Rothschild, R. Sanches, N.A. Clark, *Methods Enzymol.* 88 (1982) 696–714.
- [14] K.J. Rothschild, M. Zagaeski, W.A. Cantore, *Biochem. Biophys. Res. Commun.* 103 (1981) 483–489.
- [15] F. Siebert, W. Maentele, *Eur. J. Biochem.* 130 (1983) 565–573.
- [16] M.S. Braiman, T. Mogi, T. Marti, L.J. Stern, H.G. Khorana, K.J. Rothschild, *Biochemistry* 27 (1988) 8516–8520.
- [17] P. Roepe, D. Gray, J. Lugtenburg, E.M.M. van den Berg, J. Herzfeld, K.J. Rothschild, *J. Am. Chem. Soc.* 110 (1988) 7223–7224.
- [18] K.J. Rothschild, D. Gray, T. Mogi, T. Marti, M.S. Braiman, L.J. Stern, H.G. Khorana, *Biochemistry* 28 (1989) 7052–7059.
- [19] J. Herzfeld, J.G. Hu, in: D.M. Grant, R.K. Harris (Eds.), *Encyclopedia of NMR*, Wiley, Chichester, 1996, pp. 862–871.
- [20] B. Aton, A.G. Doukas, R.H. Callender, B. Becher, T.G. Ebrey, *Biochemistry* 16 (1977) 2995–2999.
- [21] R.A. Mathies, S.W. Lin, J.B. Ames, W.T. Pollard, *Annu. Rev. Biophys. Chem.* 20 (1991) 491–518.
- [22] K.J. Rothschild, Y.W. He, S. Sonar, T. Marti, H.G. Khorana, *J. Biol. Chem.* 267 (1992) 1615–1622.
- [23] Y. Yamazaki, M. Hatanaka, H. Kandori, J. Sasaki, W.F.J. Karstens, J. Raap, J. Lugtenburg, M. Bizounok, J. Herzfeld, R. Needleman, J.K. Lanyi, A. Maeda, *Biochemistry* 34 (1995) 7088–7093.
- [24] W. Karstens, H. Berger, E. van Haren, J. Lugtenburg, J. Raap, *J. Labelled Comp. Radiopharm.* 36 (1995) 10777.
- [25] T.S. Russell, M. Coleman, P. Rath, A. Nilsson, K.J. Rothschild, *Biochemistry* 36 (1997) 7490–7497.
- [26] R.A. Mathies, *Proc. Indian Acad. Sci. Chem. Sci.* 103 (1991) 283–293.
- [27] K.J. Rothschild, T. Marti, S. Sonar, Y.W. He, P. Rath, W. Fischer, O. Bousché, H. Khorana, *J. Biol. Chem.* 268 (1993) 27046–27052.
- [28] M. Coleman, A. Nilsson, T.S. Russell, P. Rath, R. Pandey, K.J. Rothschild, *Biochemistry* 34 (1995) 15599–15606.
- [29] D. Oesterhelt, W. Stoeckenius, *Methods Enzymol.* 31 (1974) 667–678.
- [30] A. Maeda, J. Sasaki, Y.J. Ohkita, M. Simpson, J. Herzfeld, *Biochemistry* 31 (1992) 12543–12545.
- [31] P. Roepe, P.L. Ahl, S.K. Das Gupta, J. Herzfeld, K.J. Rothschild, *Biochemistry* 26 (1987) 6696–6707.
- [32] M.J. Frisch, G.W. Trucks, H.B. Schlegel, P.M.W. Gill, B.G. Johnson, M.A. Robb, J.R. Cheeseman, T. Keith, G.A. Petersson, J.A. Montgomery, K. Raghavachari, M.A. Al-La-

- ham, V.G. Zakrzewski, J.V. Ortiz, J.B. Foresman, C.Y. Peng, P.Y. Ayala, B. 2nd edn., Gaussian, Pittsburgh, PA, 1995.
- [33] M. Tanaka, *Nippon Kagaku Zasshi* 83 (1962) 657–660.
- [34] B. Hessling, G. Souvignier, K. Gerwert, *Biophys. J.* 65 (1993) 1929–1941.
- [35] O. Bousché, M. Braiman, Y.W. He, T. Marti, H.G. Khorana, K.J. Rothschild, *J. Biol. Chem.* 266 (1991) 11063–11067.
- [36] A. Maeda, J. Sasaki, Y. Shichida, T. Yoshizawa, *Biochemistry* 31 (1992) 462–467.
- [37] W. Fischer, S. Sonar, T. Marti, H.G. Khorana, K.J. Rothschild, *Biochemistry* 33 (1994) 12757–12762.
- [38] M.S. Braiman, T. Mogi, L.J. Stern, N.R. Hackett, B.H. Chao, H.G. Khorana, K.J. Rothschild, *Proteins Struct. Funct. Genet.* 3 (1988) 219–229.
- [39] S. Sonar, C.P. Lee, M. Coleman, N. Patel, X. Liu, T. Marti, H.G. Khorana, U.L. Rajbhandary, K. Rothschild, *Nature Struct. Biol.* 1 (1994) 512–517.
- [40] T. Marti, H. Otto, T. Mogi, S.J. Rosselet, M.P. Heyn, H.G. Khorana, *J. Biol. Chem.* 266 (1991) 6919–6927.
- [41] L.S. Brown, J. Sasaki, H. Kandori, A. Maeda, R. Needleman, J.K. Lanyi, *J. Biol. Chem.* 270 (1995) 27122–27126.
- [42] R. Govindjee, E.S. Imasheva, S. Misra, S.P. Balashov, T.G. Ebrey, N. Chen, D.R. Menick, R.K. Crouch, *Biophys. J.* 72 (1997) 886–898.
- [43] S. Misra, R. Govindjee, T. Ebrey, J. Chen, R. Crouch, *Biochemistry* 36 (1997) 4875–4883.